Fracture regularity of corn kernel and stalk based on fractal theory

Xingping Li*, Junyi Wang, Yanan Li, Shendi Xu, Jiarui Hou

(*School of Agricultural Equipment Engineering, Henan University of Science and Technology, Luoyang 471003, Henan, China*)

Abstract: Since the fracture property of corn stalk determines the difficulty for corn to fall off, it is of great significance to study the fracture law of the corn stalk with high water content and explore the corn threshing method without causing great damage. Taking two varieties of corn as the research object, this study carried out single and multi-angle corn stalk fracture tests to explore the changes in the linkage between stalk and corn kernel at different positions as well as under different application modes and angles. The results showed that the force required for radial stretching was the greatest. Moreover, the fracture mechanics model of corn stalk was established to measure the fracture toughness of corn stalk. The peak value of critical load P_Q load displacement curve (F_{MAX}) was indicated. Based on the fractal theory, the fractal characteristics of the fracture surface of the stalk at different positions of the ear were analyzed, and the fractal dimension was calculated using the islet method. The findings indicated that the larger the fractal dimension of the fracture surface on the corn stalk, the more energy consumed in the fracture of corn stalk. These findings can be further utilized to explore the performance of corn kernel and reveal the fracture rule of corn kernel and stalk to identify the optimal form of force to make corn kernels fall off the corn cob and provide the theoretical basis for reducing the loss caused in the falling process of corn kernel.

Keywords: corn kernel, force of connection, fracture law, fractal characteristics, fractal dimension

DOI: 10.25165/j.ijabe.20251803.9222

Citation: Li X P, Wang J Y, Li Y N, Xu S D, Hou J R. Fracture regularity of corn kernel and stalk based on fractal theory. Int J Agric & Biol Eng, 2025; 18(3): 37–43.

1 Introduction

Corn, as an important source of food, has been playing an essential role in feed, food, chemical, and medical industries[1]. With the rapid development of society[2], mechanization has become the inevitable path for the development of corn[3-5], and corn mechanical harvesting technology will move towards directly harvesting corn kernels. Corn will have complex mechanical contact with the threshing machinery components in the threshing process, including extrusion, collision, friction, etc.[6], during which kernel crushing rate and loss rate[7] are greatly affected by the quality of the threshing device[8].

Corn threshing has been extensively studied in China and overseas[9]. Using an in-situ compression testing device, Yan et al.[10] performed in-situ compression tests on corn kernels and observed the change in their microscopic morphology in real time. Through compression tests, Singh et al.[11] obtained the mechanical characteristic images of corn kernels with different water contents and calculated elastic modulus, ultimate compression stress, and other parameters, finding that all the above parameters decreased with the increase of water content. Li et al.[12] explored the compression characteristics of corn and the law of crack formation in corn kernels through static compression tests. Srison et al.[13,14] explored the factors affecting the loss and power consumption of axial-flow corn threshing equipment and ultimately found that the gaps between nail teeth, between tapered rod and concave plate, as well as between concave plates, had a significant impact on the loss and power consumption of the thresher, but no significant effect on the fracture rate of corn kernels[15]. Geng et al.[16] designed a cross-axial flow flexible corn threshing device with a built-in flexible threshing cylinder, in which the threshing element adopts a combination structure of flexible nail teeth and elastic short grain rod to thresh corn ears flexibly without great damage[17]. The corn threshing experiment consumes much time and energy and is limited by seasons and space. The simulation technology can be used to parameterize material[18], threshing device, and operation parameters and analyze the operation mechanism[19,20]. Dai et al.[21] designed a variable diameter variable spacing seed corn threshing test bench to dynamically adjust feed amount, threshing device speed, threshing unit spacing, and other parameters and verified the process using simulation software. The simulation results were consistent.

Therefore, the objective of this research is to reduce the damage rate of corn with high water content in the threshing process[22]. In the present study, the fracture rule of corn stalk with high water content was examined. On the basis of the single corn stalk fracture test, triaxial fracture test and multi-angle stalk shear test were carried out. Based on the test results, the fracture mechanics model of corn kernel stalk was established, and the fracture toughness of corn kernel stalk was measured. Based on the fractal theory, the fractal characteristics of the fracture surface of the stalk at different positions of the ear were analyzed so as to identify the optimal form of force to make corn kernels fall off the corn cob.

2 Analysis on the fracture rule of corn kernel stalk

2.1 Fracture rule of corn kernel stalk under different influencing factors

The fracture mechanism of a single corn kernel was studied to provide a theoretical basis for analyzing the force and motion law of

Received date: 2024-07-14 **Accepted date:** 2025-01-14

Biographies: Junyi Wang, MS, research interest: crop harvesting machinery Email: 15139042158@163.com; **Yanan Li**, PhD, research interest: crop harvesting machinery, Email: LI1516359758@126.com; **Shendi Xu**, MS, research interest: crop harvesting machinery Email: lwzyzjz@163.com; **Jiarui Hou**, MS, research interest: crop harvesting machinery Email: rjdj888813@163.com.

***Corresponding author: Xingping Li**, Professor, research interest: crop harvesting machinery. Collage of Agricultural Equipment Engineering, Henan University of Science and Technology, Luoyang 471003, Henan, China. Tel: +86-13592065522, Email: aaalxp@126.com.

multiple corn kernels in the threshing process. The corn ear was divided into upper, middle, and lower segments. The segmentation diagram of the corn ear is shown in Figure 1. The external force resulting in the complete fracture of the stalk originated from stalk connection. The fracture performance of the stalk determines the difficulty for corn kernels to fall off the corn cob under the action of external force[23]. Therefore, the research on the fracture performance of kernels and stalks reveals the fracture rule of corn kernels and provides a theoretical basis for the shedding of corn kernels with a lower loss rate[24].

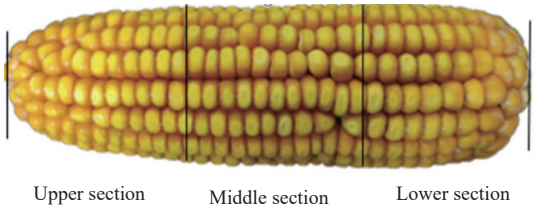

Figure 1 Segmentation diagram of corn ear

Two varieties of corn, namely Boyun 88 and Zhengdan 958, were used as the research object. The measured average water content of the two varieties was 34.2% and 31.37%, respectively. The fracture test bench of corn stalk was built according to the shape of the corn ear, as shown in Figure 2a. The test bench was composed of a texture analyzer, grain fixture, and corn ear clamping device. As shown in Figure 2b, the corn ear holding device comprised a frame, a sliding table, and a corn ear holding claw.

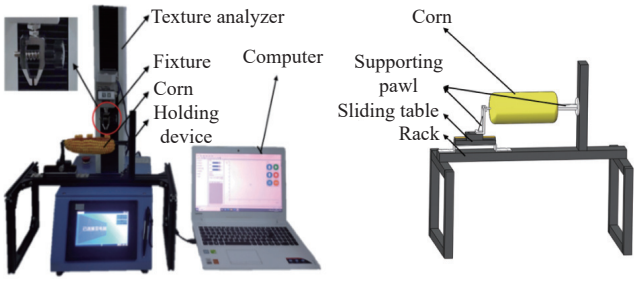

a. Test bench for the fracture of corn stalk b. Corn ear holding device

Figure 2 Fracture test on the carpopodium of the corn kernel

The single-factor experiment was conducted, with the external force applied to the corn kernel in the axial direction of the corn ear. The spatial coordinate system of the corn ear was constructed, as shown in Figure 3. The connection between the kernel and the corn cob, that is, the stalk, is denoted as the origin *O*. The connection between the origin *O* and the top of the kernel is denoted as the *Z*-axis, while the corn cob is denoted as the *X*-axis and the tangent of the outer surface of the corn cob as the *Y*-axis. The forces were applied through radial stretching, axial shearing, and tangential shearing, respectively, in the *Z*-, *X*-, and *Y*-axes in the coordinate system, as shown in Figure 3. The corn ear was segmented based on the position of the corn kernel, as shown in Figure 1. The connection force of the stalk served as the test indicator.

The test steps are listed as follows:

(1) Selected the corn kernels to be tested on the corn ear.

(2) Removed the kernels around the selected corn kernels to be tested.

(3) Used a clamping device to fix the corn ear on which the test was to be performed.

When the force was applied through radial stretching, the corn kernel fixture was moved to an appropriate position by the texture analyzer, and then the kernel to be measured was held by the fixture. When the force was applied through axial and tangential shear, the corn grain gripper was replaced with an indenter, and then the indenter was moved to an appropriate position. The force was applied immediately after the corn ear was fixed, and a high-speed camera was used to record the fracture process of the corn stalk. The forces were applied through radial stretching, axial shear, and tangential shear.

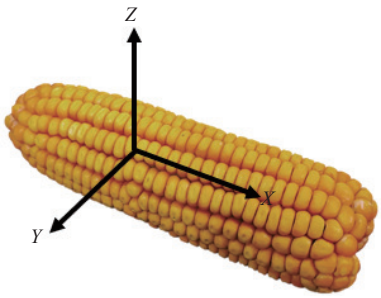

Figure 3 Triaxial coordinate diagram of corn ear

It can be concluded that at the exact position of the corn ear, the force required for complete shaft fracture under radial stretching was much greater than that under tangential and axial shear, and the force measured under tangential shear was slightly greater than that measured under axial shear. To facilitate the mechanical analysis of the fracture process of the corn kernel stalk, the shape of the stalk was simplified into a cone (Figure 4).

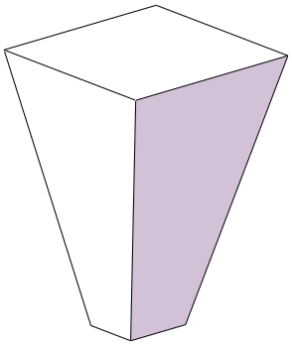

Figure 4 Simplified diagram of corn kernel stalk structure

The whole section was stressed evenly when the corn kernel was subjected to radial stretching. The force on the edge of the section was the largest when the corn kernel was subjected to shear. Therefore, every single point of the stalk section reached the limit under the action of radial stretching, while only the outermost part reached the limit under the action of shear. Hence, the force required for the stalk to break under radial stretching was much greater than that required under the action of shear. Under the same application mode, the stalk connection relay of the corn kernel in the upper part of the ear was the smallest, while that in the middle part of the ear was the largest, with a slight difference among the three segments of the ear. With the increase of the angle between the external force and the *Z*-axis of the corn ear, the force required for the fracture of the corn kernel stalk became smaller (The device is shown in Figure 5).

2.2 Mechanical analysis and model establishment of corn stalk fracture process

This section details the mechanical analysis and model establishment of stem fracture in axial and tangential shear. A high-speed camera was used to photograph the fracture process of the

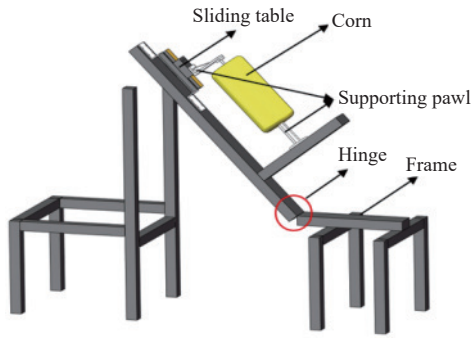

Figure 5 Multi-angle corn ear holding device

corn kernel stalk under the action of axial and tangential shear, and the motion trajectory of the corn kernel was plotted using the central position of the top surface of the corn kernel as a reference point.

As shown in Figure 6, the corn kernel rotated around the handle in the loading process simultaneously. To facilitate analysis, the motion path of the corn kernel was simplified into a straight line with a specific angle relative to the motion path of the indenter. Figure 6 shows the forces and motion trajectories of the corn kernel under the action of axial and tangential shear.

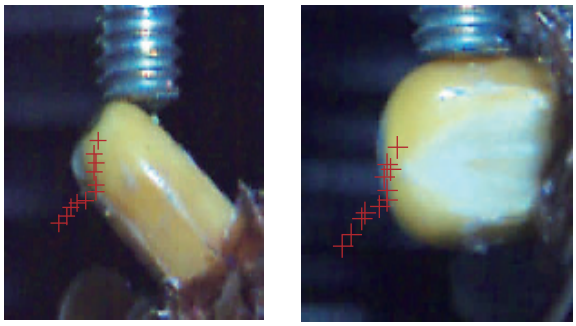

a. Axial shear b. Tangential shear

Figure 6 Motion trajectories of corn kernel

In Figure 7a, *X*-axis and *Z*-axis are the coordinate axes in the three-axis coordinate system of the corn ear; F_C is the connecting force of the stalk; F_{CX} and F_{CZ} are the two component forces in the *X*-axis and *Z*-axis direction of F_C, respectively; H_1 and L_1 are the displacement of the indenter and that at the stress point after the fracture of the handle for the corn kernel; θ_1 is the angle between the axis (*X*-axis) of the corn ear and the horizontal plane (the angle between the external force and the *Z*-axis of the corn ear); α_1 is the angle between the reduced motion path of the corn kernel and the motion path of the indenter; and β_1 is the angle between the reduced motion path of the corn kernel and the *X*-axis.

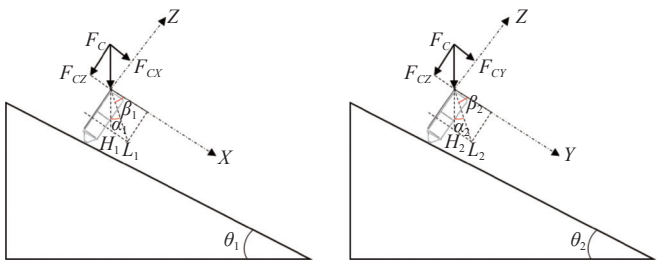

a. Axial shear b. Tangential shear

Figure 7 Schematic diagram of force and motion trajectories of corn kernel under force

In Figure 7b, *Y*-axis and *Z*-axis are coordinate axes in the three-axis coordinate system of the corn ear; F_C is the shank connection; F_{CY} and F_{CZ} are the two component forces in the *Y*-axis and *Z*-axis direction of F_C, respectively; H_2 and L_2 are the displacement of the indenter and that at the stress point after the fracture of the handle for the corn kernel; θ_2 is the angle between the *X*-axis of the corn ear and the horizontal plane (the angle between the external force and the *Z*-axis of the corn ear); α_2 is the angle between the reduced motion trajectory of the corn kernel and the motion trajectory of the indenter; and β_2 is the angle between the reduced motion trajectory of the corn kernel and the *X*-axis.

It can be seen from Figure 7a that the axial shear force exerted on the corn kernel could be decomposed into two forces in the negative direction of the *Z*-axis and the positive direction of the *X*-axis, of which the latter played a vital role in the fracture of the corn kernel stalk. When a single corn kernel was subjected to axial shear along the *X*-axis, the stress on the fruit stalk was considered a single-degree-of-freedom vibration system. The simplified model is shown in Figure 8a. It can be seen from Figure 7b that the tangential shear force exerted on the corn kernel could be decomposed into two forces in the negative direction of the *Z*-axis and the positive direction of the *Y*-axis, of which the latter played a critical role in the fracture of the corn kernel stalk. When a single corn kernel was subjected to tangential shear along the *Y*-axis, the stress on the fruit stalk was regarded as a single-degree-of-freedom vibration system, as shown in Figure 8b.

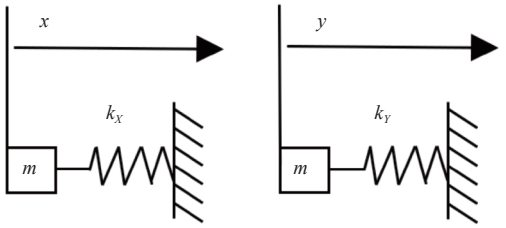

a. Simplified mechanical model of the carpopodium under the action of F_{CX} b. Simplified mechanical model of the carpopodium under the action of F_{CY}

Figure 8 Simplified mechanical model of the carpopodium under the action of F_C

In Figure 8a, k_X and k_Z are the stiffness coefficients of corn stalks in the *X*-axis and *Z*-axis directions, respectively, and *x* is the displacement component of corn stalks in the *X*-axis direction.

The physical parameter model of this system is expressed as

$$m\ddot{x} - k_X x = f(t) \tag{1}$$

where, *m* ismass of a single corn kernel; k_X is stiffness coefficient of the corn kernel stalk in *X*-axis direction; *x* and $\ddot{x}$ are displacement component and acceleration of the corn kernel in *X*-axis direction, respectively; *t* is time; and *f*(*t*) is exciting force.

If $f(t) = 0$, Formula (1) can be written as

$$m\ddot{x} - k_X x = 0 \tag{2}$$

where, $m\ddot{x} = F_{CX}$, the component of the axial shear force exerted on corn grains on the *X*-axis can be obtained by

$$F_{CX} = k_X x \tag{3}$$

According to the geometric relationship in Figure 8, It can be obtained:

$$\begin{cases} x = L_1 \cos\beta_1 \\ z = L_1 \sin\beta_1 \\ H_1 = L_1 \cos\alpha_1 \end{cases} \tag{4}$$

$$\begin{cases} \alpha_1+\beta_1+\theta_1=\dfrac{1}{2} \\ \tan\beta_1=\dfrac{z}{x} \end{cases} \tag{5}$$

$$\tan\theta_1=\frac{F_{CX}}{F_{CZ}}=\frac{k_X x}{k_Z z} \tag{6}$$

where, x and z are the displacement components of displacement L at the stress point of corn stalk fracture along the X-axis and Z-axis; k_Z are the stiffness coefficients of the corn stalk along the Z-axis; and F_{CX} and F_{CZ} are the components of external forces F_C along the X-axis and Z-axis, respectively.

According to Equations (4)-(6), the displacement component of the corn kernel along the X-axis can be obtained as

$$x=H_1\frac{\cos\beta_1}{\cos\alpha_1}=H_1\frac{\cos\left(\dfrac{k_X}{k_Z}\tan^{-1}\theta_1\right)}{\sin\left(\theta_1+\dfrac{k_X}{k_Z}\tan^{-1}\theta_1\right)} \tag{7}$$

Substituting Equation (7) into (3), the component of the axial shear force exerted on the corn kernel in X-axis can be obtained as

$$x=H_1\frac{\cos\beta_1}{\cos\alpha_1}=H_1\frac{\cos\left(\dfrac{k_X}{k_Z}\tan^{-1}\theta_1\right)}{\sin\left(\theta_1+\dfrac{k_X}{k_Z}\tan^{-1}\theta_1\right)},\ 0<\theta_1\le\frac{\pi}{2} \tag{8}$$

As can be seen from the above formula, F_{CX} will decrease with the increase of θ, which indicates that the closer the angle between the external force and the Z-axis of the corn ear is to 90°, the easier the corn kernel stalk is to break.

According to the analysis process of axial shear, the tangential shear was solved, and the component of the tangential shear force applied to the corn kernel on the X-axis was finally obtained as

$$F_{CY}=k_Y H_2\frac{\cos\left(\dfrac{k_Y}{k_Z}\tan^{-1}\theta_2\right)}{\sin\left(\theta_2+\dfrac{k_Y}{k_Z}\tan^{-1}\theta_2\right)},\ 0<\theta_2\le\frac{\pi}{2} \tag{9}$$

It can be seen from the above formula that F_{CY} will decrease with the increase of θ, which indicates that the closer the angle between the external force and the Z-axis of the corn ear is to 90°, the easier the corn kernel stalk is to break.

3 Fractal characteristics and fractal dimension of the fracture surface of corn stalk

3.1 Fractal characteristics of the fracture surface of corn stalk

Fractal theory, proposed by Mandelbrot, is a scientific method used to understand the whole from the part by observing the fine structure in the complex phenomenon by the self-similarity principle. The most essential features of the fractal theory are self-similarity and fractal dimension (fractal dimension value)[25]. The former is a criterion used to determine if an object belongs to a fractal structure, and the latter is a quantitative value to describe the complexity of an object. The fracture surface of an object exhibits random or statistical self-similarity in the event of fracture. Therefore, fractal theory can be applied to analyze the characteristics of the fracture surface, and the degree of irregularity can be described by calculating the fractal dimension of the fracture surface[26]. The effect of corn kernel position on stalk connection can be analyzed by calculating the fractal dimension of the corn kernel stalk at different positions.

The fracture toughness of corn stalk reflects the resistance to crack development when the stalk breaks under the action of external force. In material fracture mechanics, cracks could be divided into opening, sliding, and tearing types (as shown in Figure 9). According to the above analysis, the fracture at the stalk was in the form of opening crack[27]. Referring to the methods in GB/T4161-2007 and ASEME399-06, the compact stretching method was used to test the fracture toughness of corn stalk *KIC*, which can be calculated by

$$K_{IC}=\frac{P_Q}{B\sqrt{W}}f\left(\frac{a}{W}\right) \tag{10}$$

$$f\left(\frac{a}{W}\right)=29.6\sqrt{\frac{a}{W}}-185.5\left(\frac{a}{W}\right)^{\frac{3}{2}}+655.7\left(\frac{a}{W}\right)^{\frac{5}{2}}-1017.0\left(\frac{a}{W}\right)^{7}+638.9\left(\frac{a}{W}\right)^{\frac{9}{2}} \tag{11}$$

where, K_{IC} is the fracture toughness of the corn kernel stalk, P_Q is the critical load, a is the maximum length of the stalk, B is the average thickness of the stalk on the side of the corn kernel, and W is the average width of the stalk on the abdomen of the corn kernel.

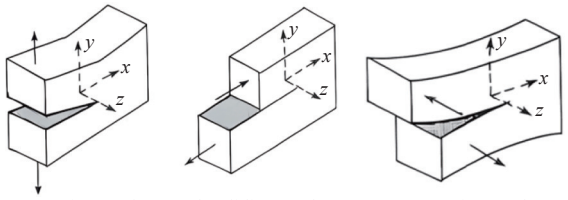

Figure 9 Three basic types of cracks

The stalk parameters in the formula are shown in Figure 10. At the same time, 40 corn kernels were selected from each segment of the two varieties of corn, and relevant parameters and stalk parameters were measured and averaged. The measurement results are listed in Table 1.

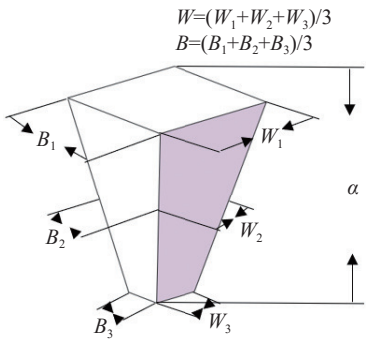

Figure 10 Definition of characteristic size of carpopodium

where, W_1 is the thickness of the upper section of the kernel and B_1 is the width of the upper section; W_2 is the thickness of the middle section of the kernel and B_2 is the width of the middle section; W_3 is the thickness of the lower section of the kernel and B_3 is the width of the lower section; and a is the height of the kernel.

Since the connection between the stalk and the clamshell of corn cob was the weakest, cracks emerged at the connection between the stalk and the clamshell under the action of external force, so it was not necessary to fabricate cracks in advance when the compact stretch method was employed to measure the fracture toughness of the corn stalk. The test principle of the compact stretching method is consistent with that of the radial stretching method applied in the fracture test of the stalk of the upper section of the corn kernel. The measured data are listed in Table 2.

Table 1 Measurement results of characteristic size of carpopodium

Seed position	Argument	Boyun 88					Zhengdan 958				
		Number of measurements			Average value	Standard deviation	Number of measurements			Average value	Standard deviation
		1	2	3			1	2	3		
Upper section	*a*	1.87	1.76	1.89	1.84	0.057	1.57	1.62	1.58	1.59	0.022
	B	1.51	1.44	1.46	1.47	0.029	1.33	1.32	1.40	1.35	0.036
	W	1.85	1.94	1.97	1.92	0.051	1.61	1.69	1.71	1.67	0.043
Middle section	*a*	1.93	1.86	1.88	1.89	0.029	1.78	1.69	1.72	1.73	0.037
	B	1.71	1.76	1.69	1.72	0.029	1.47	1.54	1.46	1.49	0.036
	W	1.78	1.74	1.67	1.73	0.045	1.71	1.80	1.77	1.76	0.037
Lower section	*a*	1.64	1.59	1.60	1.61	0.022	1.73	1.68	1.75	1.72	0.029
	B	1.66	1.62	1.76	1.68	0.059	1.58	1.48	1.56	1.54	0.043
	W	1.67	1.61	1.67	1.65	0.028	1.83	1.75	1.73	1.77	0.043

Table 2 Measurement results of radial tension of carpopodium

Varieties of corn	Boyun 88			Zhengdan 958		
Seed position	Upper section	Middle section	Lower section	Upper section	Middle section	Lower section
Load F_C/N	8.41	10.62	9.86	8.65	10.71	10.28
	8.78	10.78	10.25	8.94	10.37	10.69
	8.67	10.16	10.28	8.42	10.84	10.23
Average value	8.62	10.52	10.13	8.67	10.46	10.40
Standard deviation	0.155	0.263	0.191	0.213	0.198	0.206

Figure 11 shows the load-displacement curve of the first test in the radial tensile test. In the initial loading stage, the joint between the stalk and the glume shell of corn kernels did not crack, and the load of the curve did not change significantly. With the progress of loading, cracks began to appear at the joint of the corn stalk and glume shell, the load-displacement curve remained straight, and the kernel unstably expanded in the aftermath of cracks. Therefore, the critical load P_Q served as the peak value of the load-displacement curve (F_{MAX}). The data in Tables 1 and 2 were substituted into Formulas 10 and 11 to calculate the fracture toughness of the corn kernel stalk, as shown in Table 3.

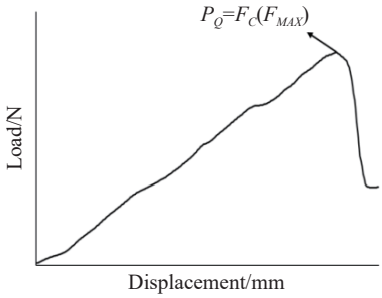

Figure 11 Schematic diagram of selection method for critical load P_Q

Table 3 Fracture toughness of carpopodium

Varieties of corn	Seed position	K_{IC}/MPa·mm$^{1/2}$
Boyun 88	Upper section	4.12×10^{-4}
	Middle section	6.51×10^{-4}
	Lower section	5.10×10^{-4}
Zhengdan 958	Upper section	4.51×10^{-4}
	Middle section	5.74×10^{-4}
	Lower section	5.51×10^{-4}

Note: K_{IC} is the fracture toughness of the corn kernel stalk.

At the end of the corn stalk fracture test, the typical corn kernels that fall off in the three regions of the corn ear were scanned to extract the outer contour of the broken surface of the corn stalk. The extracted outer contour was the fractal curve of the fractured surface of the corn stalk, as shown in Figure 11. The fractal curve of the fracture surface of the stalk was complex and randomly distributed, endowing it with irregular self-similar characteristics, as well as nonlinear characteristics in the spatial distribution. According to the fractal pattern property, the fracture surface of the corn kernel stalk exhibited a random quasi-order structure, which reflects a certain degree of self-similarity, so the fracture of the corn kernel stalk was identified to be in the form of a fractal structure. Figures 12a-12c respectively show corn kernels at the top, middle, and bottom of the corn ear.

a. Upper segment region b. Middle segment region c. Lower segment region

Figure 12 Fractal curve of fracture surface of carpopodium

As can be seen from Figure 12, the fractal curves of the fracture surface of the kernel stalk in the three regions were spike-like, nested with small "spike-like" curves, and the whole crack path formed a self-similar multi-level structure. The fractal curve of the fracture surface of the corn stalk in the middle region was more complex, the cracks growing at the fracture were distributed in a more complicated manner, and the distribution of the curve in the plane demonstrated more obvious nonlinear characteristics.

3.2 Fractal dimension value of fracture surface of corn stalk

The islet and vertical profile contour methods are mainly used for calculating fractal dimension. Corn kernels were firstly scanned in a three-dimensional manner. Then, the islet method was used to calculate the fractal dimension of the fracture surface of the corn kernel stalk. The fractal dimension at different locations was statistically analyzed to investigate its influence on the mechanical properties[28]. The measurement process of the fractal dimension of the fracture surface of the corn stalk is depicted as follows:

1) Extraction of three-dimensional model of kernel stalk

A three-dimensional scanner was used to scan the corn kernel and extract its external surface features. The three-dimensional model data of the corn stalk was obtained, as shown in Figure 13. Figure 13a-13c display the corn kernel scanning model in the upper, middle, and lower segment regions of the corn ear.

Following that, the file was imported into the UG_NX software, and the three-dimensional model of the corn kernel was edited, with the corn kernel stalk left, as shown in Figure 14. Figure 14a, b, and

c is a three-dimensional model of the stalk in the upper, middle, and lower segment regions of the corn ear, respectively.

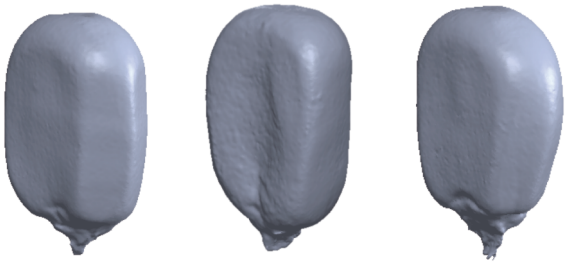

a. Upper segment region b. Middle segment region c. Lower segment region

Figure 13 Three-dimensional model of corn kernels

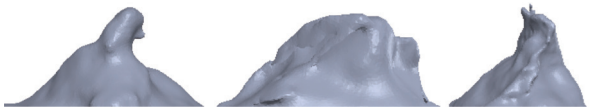

a. Upper segment region b. Middle segment region c. Lower segment region

Figure 14 Three-dimensional model of carpopodium

2) Acquisition of parameters for calculation of fractal dimension values

A shear plane (as shown in Figure 15) parallel to the projection plane at the crack of the fruit stalk was established. The positions that coincided with the top and bottom of the fruit stalk (Point A) were respectively set as the initial and final positions. The vertical distance between the two is h.

Isometric shear was performed on the three-dimensional model of the stalk at N times (N≥6) between the initial and final positions, and the spacing between two adjacent shear planes can be expressed as

$$n = \frac{h}{N+1} \tag{12}$$

where, n is an integer and meets $n\cdot(N+1)\leq h$; the unit is μm.

In the process of cutting corn stalks, the distance between the shear plane used for the i(i=1, 2, ..., N) shearing and the initial position was denoted as L_i, and the cross-section area obtained after the stalks were cut was denoted as S_i (S_i measured by software). Take the logarithms of L_i and S_i to get lnL_i and lnS_i. With lnL_i as the independent variable, lnS_i as the dependent variable, and with N shear N group get lnL_i and lnS_i fitting[29,30], get the linear relation between the two as follows:

$$\ln S_i = D_s \ln L_i + C \tag{13}$$

where, D_s is the fractal dimension of the stalk fracture, and C is the fitting constant.

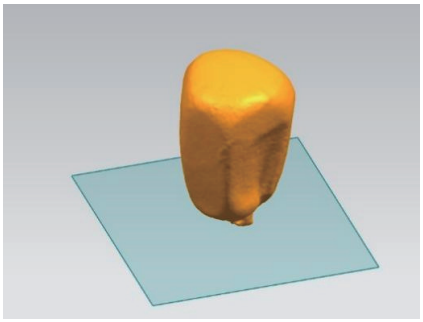

Figure 15 Initial cutting plane

According to the above method, the corn kernel stalks were scanned, and the cross-sectional areas of each stalk were measured. The distance between adjacent cross-sectional areas was 150 μm. Figure 16 shows the typical cross-sectional shapes of corn kernel stalks.

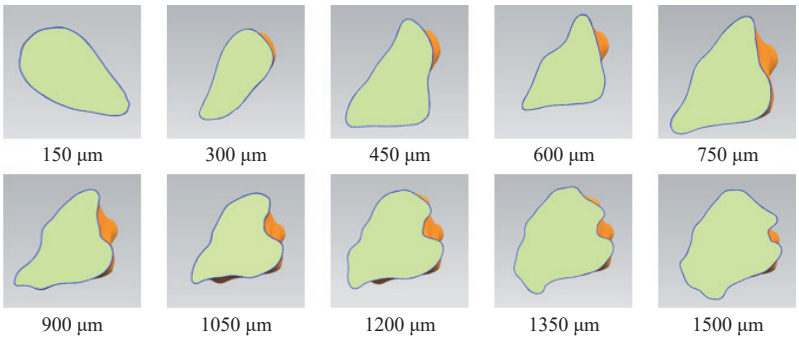

Figure 16 Cross-sectional shapes at the fracture of carpopodium

The lnL_i and lnS_i values of corn kernels in the three regions of the corn ear were measured and fitted, and the linear fitting diagrams of lnL_i and lnS_i of kernel stems in different ear regions were obtained (Figure 17). Figure 17 shows the linear fitting diagram of fractal dimension values of corn kernels in the three regions of the corn ear.

It can be concluded from the linear fitting results of lnL_i and lnS_i that the fractal dimensions of the fracture surface of the kernel stalk in the upper, middle, and lower segments of the corn ear were 1.2103, 1.5755, and 1.400, respectively. In combination with the above stalk fracture test results, the more complex the surface structure of the fracture of corn kernel stalks and the larger the fractal dimension of the stalk fracture surface, the more energy would be consumed for the stalk to fracture, and therefore the more significant the external force required for the stalk to fracture.

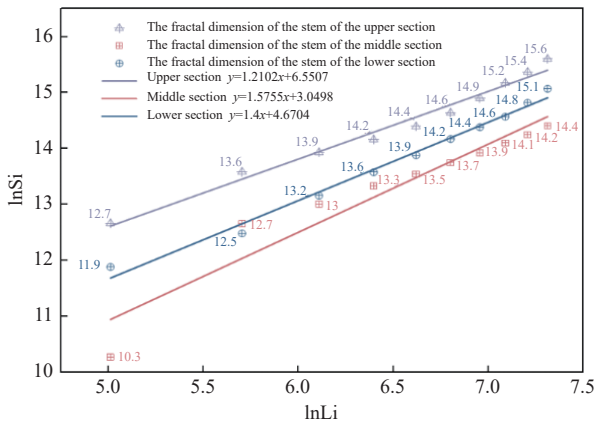

Figure 17 Linear fitting graph of lnL_i and lnS_i

4 Conclusions

1) A corn ear clamping device and a corn stalk fracture test rig were prepared. This article explored the influence of kernel position, force application method, and angles on the corn kernel stalk connection force through single-kernel and multi-angle stalk fracture tests. At the same position as the corn ear, the force required for shaft fracture under radial stretching was much larger than that under tangential and axial shear, and the force measured under tangential shear was slightly larger than that under axial shear. With the increase of the angle between the external force and the *Z*-axis of the corn ear, the force required to fracture the stalk became smaller.

2) The fracture mechanics model of the kernel and shank was established according to the fracture test of the kernel and shank, and the boundary conditions for the fracture of the kernel and shank were established. Under axial shear, the stress of the shank was regarded as a single-degree-of-freedom vibration system, and F_{CX} decreased with the increase of θ. The closer the angle between the external force and the *Z*-axis of corn ear was to 90°, the easier it was to break the kernel stalk. Under tangential shear, the stress on the stalk was also considered a single-degree-of-freedom vibration system, and F_{CY} decreased with the increase of θ. The closer the angle between the external force and the *Z*-axis of the corn ear was to 90°, the easier it was for the stalk to break.

3) The fracture toughness of corn kernels was measured. The fractal theory was applied to analyze the characteristics of the fracture surface of the material, and the degree of irregularity was described by calculating the fractal dimension of the fracture surface. Based on the fractal theory, the fractal characteristics of the stalk fracture surface at different positions of the corn ear were analyzed, and the fractal dimension of the fracture surface of the corn kernel stalk was calculated by the islet method. The results showed that the more complex the surface fracture structure of the corn stalk, the larger the fractal dimension of the stalk fracture surface, and the more energy would be consumed by the stalk fracture, and therefore, the more significant the external force required to cause the stalk to fracture.

Acknowledgements

This work was supported by the National Natural Science Foundation of China (Grant No. 52275245) and Henan Science and Technology Research Program (Grant No. 222103810041).

[References]

[1] Yang J Y, Li X, Xie Y, Wang N, Liu W C. Anti-hepatoma activity and mechanism of corn silk polysaccharides in H22 tumor-bearing mice. International Journal of Biological Macromolecule, 2014; 64: 276–280.

[2] Li S K, Wang K R, Xie R Z, Hou P, Ming B, Yang X X, et al. Implementing higher population and full mechanization technologies to achieve high yield and high efficiency in maize production. Crops, 2016; 4: 1–6. (in Chinese)

[3] Ouyang A, Fan C L, Zhao H, Dong J Q, Jiao Y X. Present status and equipment research progress of maize full mechanized production. Journal of Chinese Agricultural Mechanization, 2022; 43(6): 207–214. (in Chinese)

[4] Li Y, Yan B X, Zhang D X, Zhang T L, Wang Y X, Cui T. Research progress on precision planting technology of maize. Transactions of the CSAM, 2016; 47(11): 38–48.

[5] Wang K R, Xie R Z, Xue J, Sun L R, Li S K. Comparison and analysis of maize grain commodity quality and mechanical harvest quality between China and the United States. Int J Agric & Biol Eng, 2022; 15(1): 55–61.

[6] Srison W, Chuan-Udom S, Saengprachatanarak K. Effects of operating factors for an axial-flow corn shelling unit on losses and power consumption. Agriculture and Natural Resources, 2016; 50(5): 421–425.

[7] Li S K, Wang K R, Xie R Z, Ming B. Mechanical kernel harvesting promoted the transformation of maize production mode. Agricultural Science in China, 2018; 51(10): 1842–1844. (in Chinese)

[8] Fan C L, Zhang D X, Yang L, Cui T, He X T, Zhao H H. Development and performance evaluation of a guide vane inclination automatic control system for corn threshing unit based on feed rate monitoring. Computers Electronics in Agriculture, 2022; 194: 106745.

[9] Li X P, Zhang W T, Xu S D, Ma F L, Du Z, Ma Y D. Calibration of collision recovery coefficient of corn seeds based on high-speed photography and sound waveform analysis. Agriculture, 2023; 13(9): 1677.

[10] Wang X, Yan H, Hou J. Study on mechanical properties of maize kernel texture puncture and in-situ compression. Anhui Agricultural Sciences, 2017; 45(11): 210–213, 249. (in Chinese)

[11] Singh S, Finner M, Rohatgi P, Buelow F, Schaller M. Structure and mechanical properties of corn kernels: a hybrid composite material. Journal of Materials Science, 1991; 26: 274–284.

[12] Li X P, Xiong S, Geng L X, Ji J T. Influence of water content on anti-pressing properties of corn ear. Transactions of the CSAE, 2018; 34(2): 25–31.

[13] Li X P, Du Z, Ma Y D. Effect of kernel moisture content to the result of bare hand threshing of corn ear interval. Applied Mechanics Materials, 2014; 644-650: 5285–5290.

[14] Astanakulov K D, Kodirov B X. Fozilov G G. Development a new type corn-sheller machine for farms in Uzbekistan. International Journal of Applied Agricultural Research, 2014; 9(2): 115–120.

[15] Srison W, Chuan-Udom S. Design factors affecting losses and power consumption of an axial flow corn shelling unit. Agriculture and Natural Resources, 2016; 38(5): 421–425.

[16] Geng D Y, He K, Wang Q, Jin C Q, Zhang G H, Lu X F. Design and experiment on transverse axial flow flexible threshing device for corn. Transactions of the CSAM, 2019; 50(3): 101–108.

[17] Li X P, Gao L X. Performance test on corn thresher with different-speed threshing parts. Transactions of the CSAE, 2009; 25(12): 102–106. (in Chinese)

[18] Zhao J L, Zhao H N, Tang H, Wang X G, Yu Y J. Bionic threshing component optimized based on MBD-DEM coupling simulation significantly improves corn kernel harvesting rate. Computers Electronics in Agriculture, 2023; 212: 108075.

[19] Khawaja A N, Khan Z M. DEM study on threshing performance of “compression–oscillation” thresher. Computational Particle Mechanics, 2022; 1-16. DOI: 10.1007/s40571-021-00456-4

[20] Li X Y, Du Y F, Liu L, Mao E R, Yang F, Wu J, et al. Research on the constitutive model of low-damage corn threshing based on DEM. Computers Electronics in Agriculture, 2022; 194: 106722.

[21] Dai F, Zhao Y M, Liu Y X, Shi R J, Xin S L, Fu Q F, Zhao W Y. Analysis and performance test on dynamic seed corn threshing and conveying process with variable diameter and spacing. Int J Agric & Biol Eng, 2023; 16(2): 259–266.

[22] Martin C L, Bouvard D, Shima S. Study of particle rearrangement during powder compaction by the discrete element method. Journal of the Mechanics, 2003; 51(4): 667–693.

[23] Li X Y, Du Y F, Guo J, Mao E R. Design, simulation, and test of a new threshing cylinder for high moisture content corn. Applied Sciences, 2020; 10(14): 4925.

[24] Sui R, Pan Y, Sun J. Research on mechanical properties of peg nodes with different maturity of peanuts. The Journal of Shandong Agriculture and Engineering University, 2019; 36(3): 25–28. (in Chinese)

[25] Deng Y S, Yao Z G, Duan B Z, Li L, Meng L Q, Zhao H L. Mechanical properties of slope protection by vetiver root using fractal theory. Transactions of the CSAE, 2024; 40(4): 147–154.

[26] Duan Q S, An J J, Mao H P, Liang D W, Li H, Wang S F, et al. Review about the application of fractal theory in the research of packaging materials. Materials, 2021; 14(4): 860.

[27] Qian J, Ma S C, Xu Y, Liang W P, Zhou B C, Li W Z. Analysis of crack stress intensity factor of sugarcane cutting based on fracture mechanics. Transactions of the CSAM, 2023; 54(S2): 101–109.

[28] Xu A, Qu J, Yin Z, Wei C. Morphological characteristics of endosperm in different regions of maize kernels with different vitreousness. Journal of Cereal Science, 2019; 87: 273–279.

[29] Yu H F, Wang Y, Gao C. A fractal model of rough surfaces based on ellipsoidal asperities. Industrial Lubrication and Tribology, 2024; 76(5): 666–677.

[30] Gang L, Wang Z H, Zou L, Zhang T, Xiao W B, Yang T L. Regulating phenol tar in pyrolysis of lignocellulosic biomass: Product characteristics and conversion mechanisms. Bioresource Technology, 2024; 409: 131259.